Monte Carlo simulation of Se_xTe_{1-x} glass structure with *ab initio* potentials

John C. Mauro

NYS College of Ceramics at Alfred University, 2 Pine Street, Alfred, New York 14802, USA and Science and Technology Division, Corning Incorporated, SP-TD-01-01, Corning, New York 14831, USA

Arun K. Varshneya

NYS College of Ceramics at Alfred University, 2 Pine Street, Alfred, New York 14802, USA

We develop model interaction potentials for the binary Se-Te system using *ab initio* molecular simulations and a cluster expansion technique. These potentials are used with classical Monte Carlo simulations to characterize the structure of Se_xTe_{1-x} glasses. The model potentials successfully reproduce the two-coordinated chainlike structure of these glasses and lead to phase separation for $x \gtrsim 0.4$.

I. INTRODUCTION

Chalcogenide glasses exhibit unique electrical and optical properties applicable to a wide range of fields, including electrical and optical switching and the transmission of infrared radiation. However, these glasses must meet requirements for thermal and mechanical properties, such as glass transition temperature, strength, and toughness in order to be suitable for many applications. Experiments have shown the promising but often puzzling behavior of chalcogenide glass properties as a function of average coordination number,[1] but there is yet to be a satisfactory theoretical explanation based on first principles. An accurate description of the interatomic potentials in chalcogenide glasses is a necessary first step in order to build such theoretical understanding. In this study, we use *ab initio* molecular modeling to derive interaction potentials for selenium and tellurium, two common constituents of chalcogenide glasses.

Previous modeling of selenium has been largely based on the semiempirical model of Oligschleger *et al.*,[2] who developed potentials for selenium following an approach similar to Stillinger, Weber, and LaViolette[3] in their model of sulfur. Combining experimental data with density functional calculations, Oligschleger developed effective two- and three-body interaction potentials that reproduce known structures and energies of selenium clusters (Se_2–Se_8). The Oligschleger model of selenium has been used to determine selenium glass structure,[4] vibrational properties,[5] and quench behavior.[6–8]

Quantum mechanical techniques such as molecular orbital theory and density functional theory[9] may be used to develop models with a greater range of applicability. Shimojo *et al.*[10–12] investigated the structure and electrical properties of fluid selenium using density functional theory; Zhang and Drabold[13,14] utilized additional localization techniques[15] to study the impact of photon absorption on the structure of amorphous selenium. In addition, Shimizu *et al.*[16] and Nakamura and Ikawa[17] performed molecular orbital calculations on amorphous selenium and found good agreement between their calculated structures and those determined by infrared or Raman spectrometry. However, none of this work at the

quantum mechanical level has attempted to derive interatomic potentials and bridge the gap to larger scale classical simulations.

There has been very little work in the modeling of elemental tellurium, and none of it has been particularly successful. Attempts at modeling tellurium with density functional theory have produced highly incorrect results,[18] such as predicting a coordination number of six for liquid tellurium instead of the correct value of two.

In this study, we use *ab initio* molecular modeling and a cluster expansion technique to derive effective interaction potentials for both elemental selenium and tellurium. We also develop *ab initio* potentials for the heterogeneous Se-Te system. Finally, we use these potentials in classical Monte Carlo simulations to investigate the structure of glasses in the Se_xTe_{1-x} system.

II. SIMULATION DETAILS

In our simulations, we employ second- and fourth-order Møller-Plesset perturbation theory[19] to calculate the energy of clusters of selenium and tellurium atoms. For our modeling of elemental selenium we use the aug-cc-pVQZ basis set of Dunning and co-workers,[20] where the acronym stands for "augmented correlation-consistent polarized valence quadruple-ζ." The aug-cc-pVQZ basis set allows for explicit representation of all 34 electrons in each selenium atom using 93 basis functions composed of 343 primitive Gaussians. This explicit representation of electrons does not scale well to very large atoms such as tellurium, which has 52 electrons per atom. In this case, we employ a small-core relativistic pseudopotential[21] in which the inner shell electrons are combined with the nucleus as an effective core. For tellurium, the $n=1,2,3$ shells are incorporated into the effective core, and the $4s^2p^6d^{10}5s^2p^4$ outer electrons are modeled explicitly. The corresponding basis set is denoted aug-cc-pVQZ-pp and contains 27 basis functions with 87 primitive Gaussians.

Unfortunately, we found that a combination of the aug-cc-pVQZ basis set for selenium with the aug-cc-pVQZ-pp basis set for tellurium in heterogeneous systems does not lead to well-converged energy values due to excessive mixing of

frozen core and valence orbitals between atoms. In order to address this problem we used the aug-cc-pVQZ-pp basis set for both tellurium and selenium in all heterogeneous simulations. The aug-cc-pVQZ-pp basis set for selenium incorporates the $n=1,2$ shells into an effective core and models explicitly the $3s^2p^6d^{10}4s^2p^4$ outer electrons. We use the GAUSSIAN 03 software[22] for all *ab initio* simulations.

In order to isolate the two- and three-body interaction potentials from the total system energy, we adopt the technique of cluster expansion[23] where the total potential of a system is the sum of the monomer energies and all combinations of higher-order interactions. Mathematically, we may write the total potential as

$$V = \sum_{i=1}^{N} V_1 + \sum_{i=1}^{N}\sum_{j\neq i}^{N} V_2(r_{ij}) + \sum_{i=1}^{N}\sum_{j\neq i}^{N}\sum_{k\neq i,j}^{N} V_3(r_{ij}, r_{jk}, \theta_{ijk}) + \cdots,$$

(1)

where V_n refers to the nth-order interaction potential. In theory, the series of interactions terminates only with the V_N term, where N is the total number of atoms in the system. However, since the magnitudes of the interactions typically decrease with increasing n (and due to computational efficiency considerations), it is common to truncate the series after the second- or third-order terms.

III. INTERACTION POTENTIALS

In order to be used in higher-level classical simulations (e.g., molecular dynamics and Monte Carlo), the *ab initio* potentials are fit to continuous functions that accurately reproduce the quantum data. While it is preferable to use fitting functions drawn from physical intuition, they do not necessarily provide the best fit for our particular systems. Here we favor forms that accurately reproduce the *ab initio* results over those that are simply more physically intuitive.

A. Two-body interaction potentials

We compute the potential energy of a two-body cluster as a function of interatomic separation distance, r_{ij}, using the MP4 level of theory. Following cluster expansion theory, the two-body interaction potential is calculated by subtracting the potentials of the isolated monomers from the total dimer potential:

$$2V_{2,ij}(r_{ij}) = V(r_{ij}) - \sum_{i=1}^{2} V_{1,i}.$$

(2)

The two-body interaction potential for the Se-Se dimer, $V_{2,Se-Se}(r_{ij})$, is plotted in Fig. 1(a). As discussed elsewhere,[24] our *ab initio* model provides a significant improvement over the semiempirical Oligschleger model[2] for selenium.

We fit the *ab initio* data using a Morse potential[25] of the form

$$V_2(r_{ij}) = D_0 e^{-2\alpha(r_{ij}-r_0)} - 2D_0 e^{-\alpha(r_{ij}-r_0)}$$

(3)
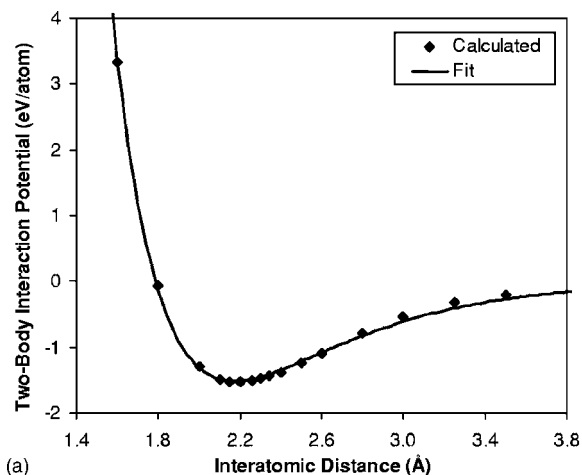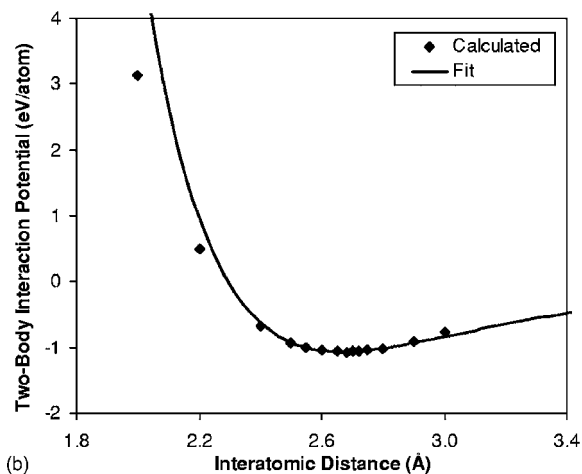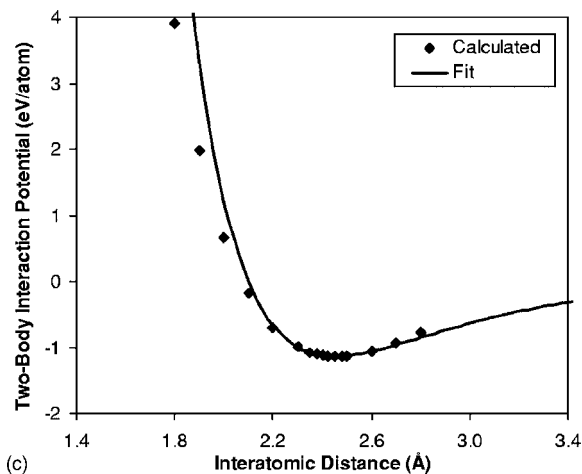
FIG. 1. Two-body (a) Se-Se, (b) Te-Te, and (c) Se-Te interaction potentials.

$$= D_0\big[\big(1 - e^{-\alpha(r_{ij}-r_0)}\big)^2 - 1\big],$$

(4)

where D_0 is the potential well depth, r_0 is the equilibrium separation distance, and α is the shape parameter. Using a least-squares fitting routine, we determine $D_0 = 1.517\,5496$ eV, $r_0 = 2.173\,4892$ Å, and $\alpha = 1.790\,2500$ Å^{-1} for the Se-Se interaction.

Please note that the *total* two-body interaction potential for a given dimer is

TABLE I. Parameters for the two-body interaction potentials.

	Se-Se	Te-Te	Se-Te
D_0 (eV)	1.517 5496	1.070 0086	1.135 9623
r_0 (Å)	2.173 4892	2.667 6502	2.449 6465
α (Å^{-1})	1.790 2500	1.852 5085	1.98 1215

TABLE II. Two-body radial parameters used in the three-body interaction potentials.

	Se-Se	Te-Te	Se-Te
b (eV$^{1/2}$)	7.907 4605	6.127 7354	19.07 6068
c (Å^{-1})	1.451 0428	1.397 2349	2.140 6499

$$V_2(r_{ij}) + V_2(r_{ji}) = 2V_2(r_{ij}). \qquad (5)$$

Thus the total cohesive energy of the Se-Se dimer is $2D_0 = 3.0351$ eV. Given a system of N atoms, the total two-body interaction potential for the ensemble is

$$V_{2,tot} = 2\sum_{i=1}^{N}\sum_{j>i}^{N} V_{2,ij}(r_{ij}). \qquad (6)$$

The two-body interaction potential for the Te-Te dimer is shown in Fig. 1(b). We fit the *ab initio* data using a Morse potential and obtain the parameters: $D_0 = 1.070\,008\,6$ eV, $r_0 = 2.667\,650\,2$ Å, and $\alpha = 1.852\,508\,5$ Å^{-1}. The fit is not quite as good at small values of r_{ij} due to the use of pseudopotentials, which for our systems tended to underestimate the repulsive energy at short separation distances where there is an increased overlap of atomic orbitals. Please note that the use of pseudopotentials has been shown to give highly accurate predictions for equilibrium separation distances and binding energies.[21,26]

Finally, the two-body interaction potential for the heteropolar Se-Te dimer is given in Fig. 1(c). Here, the optimized Morse parameters are $D_0 = 1.135\,962\,3$ eV, $r_0 = 2.449\,646\,5$ Å, and $\alpha = 1.981\,215$ Å^{-1}. A summary of all

the Morse parameters is provided in Table I. Since the Se-Te bonding energy is less than the average of the Se-Se and Te-Te bonding energies, there should be a preference for homopolar bonding in the heterogeneous Se-Te system.

B. Three-body interaction potentials

In order to calculate the three-body interaction potentials for the Se-Te system, we compute the total potential energies of the Se-Se-Se, Te-Te-Te, Se-Te-Se, Se-Se-Te, Te-Se-Te, and Se-Te-Te trimers using the MP2 level of theory. The three-body interaction is isolated by subtracting the one- and two-body contributions:

$$V_{3,ijk}(r_{ij}, r_{jk}, \theta_{ijk}) = V(r_{ij}, r_{jk}, \theta_{ijk}) - \sum_{i=1}^{3} V_{1,i} - 2\sum_{i=1}^{3}\sum_{j>i}^{3} V_{2,ij}(r_{ij}),$$
$$(7)$$

where r_{ij} is the separation distance between atoms i and j, r_{jk} is the separation between atoms j and k, and θ_{ijk} is the bond angle. Following the examples of Stillinger[3] and Oligschleger,[2] we fit the three-body interaction potentials using a separable function,

TABLE III. Fourier coefficients for the three-body angular potentials.

	Se-Se-Se	Te-Te-Te	Se-Te-Se	Se-Se-Te	Te-Se-Te	Se-Te-Te
a_0	1.473 7009	6.381 5150	19.26 4535	9.161 9754	22.22 3224	7.297 9673
a_1	−0.748 8205	−7.293 8000	−17.273 420	−10.112 3940	−13.46 2698	−10.259 955
a_2	−0.3235095	−0.8722934	−2.4874198	−2.6299683	5.2217488	−5.0139178
a_3	−0.8336347	−5.3866029	−11.597780	−5.2549641	0.520 2633	−8.6622940
a_4	0.366 1849	−1.1660934	1.338 1763	0.745 1214	4.720 5673	−0.2471748
a_5	0.055 9816	−1.4283849	−0.0107653	0.000 9848	−5.6671392	0.223 3760
a_6	0.050 6636	−0.2498004	−0.0344267	0.050 9585	−2.3424787	0.558 9294
a_7	−0.0042692	0.215 2772	−1.7371929	0.265 5886	2.786 5778	0.205 8917
a_8	−0.0116419	0.606 1612	0.321 2924	0.774 1911	2.973 9254	−0.0053356
a_9	−0.0636407	−0.0489911	2.0171 056	−0.1361319	−0.5264682	−1.6691366
a_{10}	−0.3031730	−1.0056510	1.261 2500	−1.1315190	−1.7323615	−3.3067562
a_{11}	−0.2478697	−1.2943361	−1.2352494	−1.1231347	0.092 1489	−3.3001658
a_{12}	−0.2017648	−0.6955193	−2.3823570	−0.3718989	1.935 3049	−1.2803732
a_{13}	0.018 6467	−0.0892812	−1.2790921	0.075 7642	1.747 6688	0.948 9806
a_{14}	−0.0517747	0.078 8748	−0.1052132	0.003 3640	0.541 9944	1.648 5507
a_{15}	0.033 7409	0.048 1918	−0.4400456	−0.0269044	0.082 8253	0.896 2156
a_{16}	−0.0149274	0.169 9672	−1.9463542	0.125 7210	0.022 4998	0.007 5327
a_{17}	0.053 7881	0.238 7772	−2.2185852	0.218 1182	−0.0360265	−0.2410890
a_{18}	−0.0063938	0.178 8512	−1.4913421	0.046 3594	−0.2454533	−0.0602311
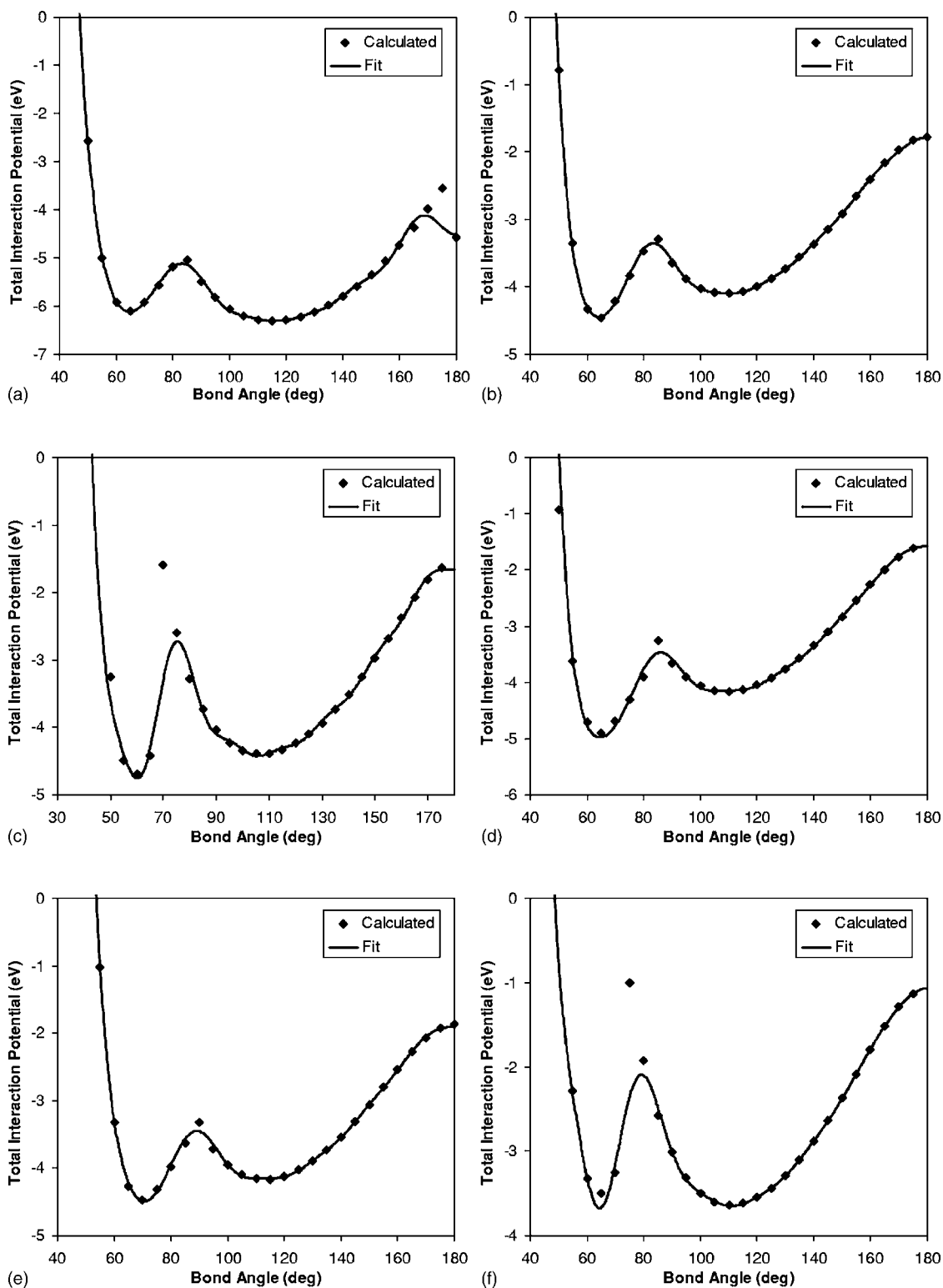
FIG. 2. Total two- and three-body interaction potentials for the (a) Se-Se-Se, (b) Te-Te-Te, (c) Se-Te-Se, (d) Se-Se-Te, (e) Te-Se-Te, and (f) Se-Te-Te trimers.

$$V_{3,ijk}(r_{ij}, r_{jk}, \theta_{ijk}) = R_{ij}(r_{ij})R_{jk}(r_{jk})\Theta_{ijk}(\theta_{ijk}). \qquad (8)$$

$$R(r) = b\,\mathrm{sech}(cr), \qquad (9)$$

For the radial components, $R_{ij}(r_{ij})$ and $R_{jk}(r_{jk})$, we adopt the form

where b and c are constants. Note that for an elemental cluster such as Se-Se-Se, $R(r) = R_{ij}(r) = R_{jk}(r)$; in a heterogeneous
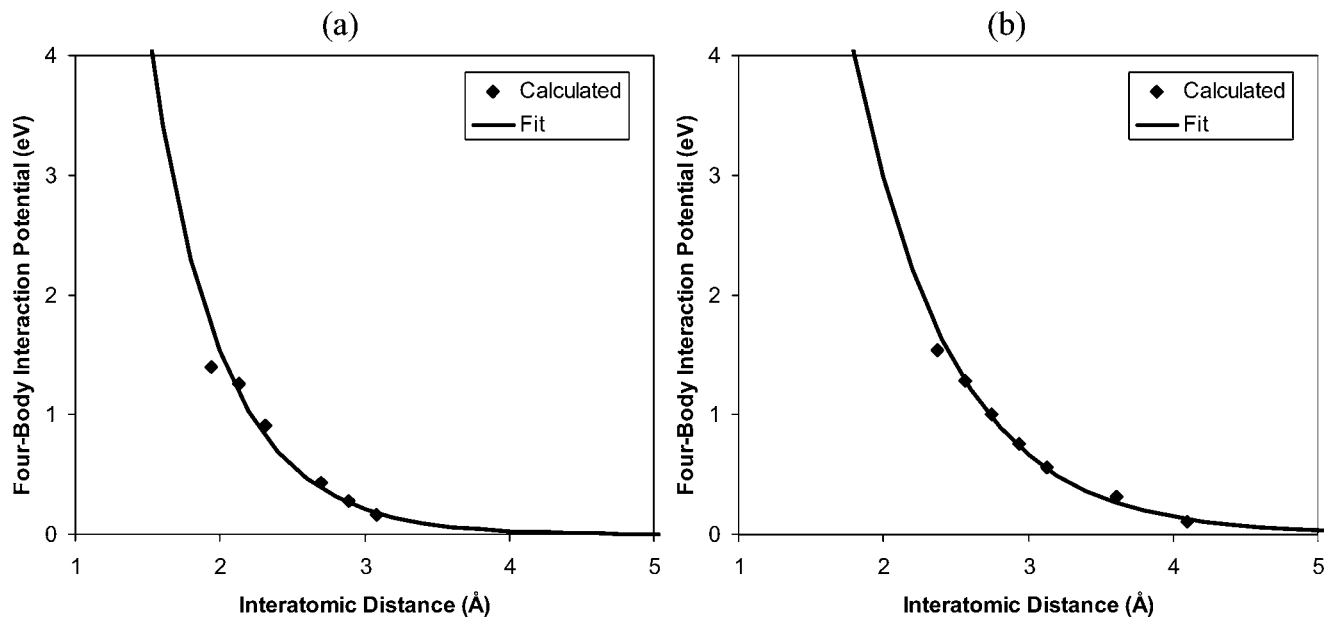
FIG. 3. Four-body interaction potentials for (a) selenium and (b) tellurium.

cluster the radial functions are defined separately for each pairwise combination of elements.

Due to symmetry reasons the angular component, $\Theta_{ijk}(\theta_{ijk})$, of the three-body potential must be an even function, so we assume a Fourier cosine solution,

$$\Theta(\theta) = \frac{1}{2}a_0 + \sum_{m=1}^{M} a_m \cos(m\theta). \qquad (10)$$

We determine the constants in the above equations by fitting the *ab initio* data using a least-square error routine. The optimized parameters for the radial and angular components are shown in Tables II and III, respectively. We truncate the Fourier series in Eq. (10) with $M = 18$ in order to provide a good fit of important features in the *ab initio* data.

Please note that in our formulation the total three-body interaction potential for any three atoms, $i, j,$ and k, is the sum of all permutations:

$$V_{3,tot} = R_{ij}(r_{ij})R_{jk}(r_{jk})\Theta_{ijk}(\theta_{ijk}) + R_{ji}(r_{ji})R_{ik}(r_{ik})\Theta_{jik}(\theta_{jik})$$
$$+ R_{ik}(r_{ik})R_{kj}(r_{kj})\Theta_{ikj}(\theta_{ikj}) + R_{ki}(r_{ki})R_{ij}(r_{ij})\Theta_{kij}(\theta_{kij})$$
$$+ R_{jk}(r_{jk})R_{ki}(r_{ki})\Theta_{jki}(\theta_{jki}) + R_{kj}(r_{kj})R_{ji}(r_{ji})\Theta_{kji}(\theta_{kji}). \qquad (11)$$

Taking into account symmetry considerations, the expression simplifies to

$$V_{3,tot} = 2R_{ij}(r_{ij})R_{jk}(r_{jk})\Theta(\theta_{ijk}) + 2R_{ij}(r_{ij})R_{ik}(r_{ik})\Theta(\theta_{kij})$$
$$+ 2R_{ik}(r_{ik})R_{jk}(r_{jk})\Theta(\theta_{jki}). \qquad (12)$$

Thus the total three-body interaction potential for the entire system is

$$V_{3,tot} = 2\sum_{i=1}^{N}\sum_{j\neq i}^{N}\sum_{k>j}^{N} V_{3,ijk}(r_{ij}, r_{jk}, \theta_{ijk}). \qquad (13)$$

The equilibrium structures for the various trimers may be determined by summing the two- and three-body interaction potentials. Figure 2 shows this total multibody interaction potential as a function of bond angle for the Se-Se-Se, Te-Te-Te, Se-Te-Se, Se-Se-Te, Te-Se-Te, and Se-Te-Te three-body clusters assuming equilibrium bond lengths for r_{ij} and r_{jk}. Whereas the minimum energy configuration for the Se-Se-Se trimer has a bond angle of 115°, the minimum energy configuration for Te-Te-Te occurs with a bond angle of 65°. The Te-Te-Te cluster has a second (relative) minimum around 110°. This "dual minimum" behavior is in good agreement with experimental cluster measurements for both selenium[2] and tellurium,[27] which predict two distinct optimized geometries: an open triangular structure and a closed, equilateral triangle. The heterogeneous trimers in Fig. 2 also exhibit minima in both the closed and open configurations.

C. Effective four-body interaction potentials

For the case of a four-body cluster we have six generalized coordinates: three interatomic separation distances, $r_{ij}, r_{jk},$ and r_{kl}; two bond angles, θ_{ijk} and θ_{jkl}; and one torsion angle, ϕ_{ijkl}. This six-dimensional phase space is much too large to explore fully at the quantum mechanical level; moreover, a full description of the four-body interaction would lead to a computation time in the classical simulation that scales as $O(N^4)$, which is impractical for systems of hundreds or thousands of atoms. Therefore, we model the four-body interaction for the Se-Te system as an effective pairwise repulsion that depends only on the separation distance between an atom and its third- and longer-distance neighbors. Computation of this effective four-body interaction in a classical simulation is on the order of $O(N^2)$, which is small compared to the $O(N^3)$ three-body calculation.

In order to determine this effective repulsion we introduce a fourth atom to the three-body clusters discussed in the pre-

vious section. We assume a bond angle of $\theta_{ijk}=60°$ and equilibrium bond lengths for the trimers. The fourth atom is positioned equidistant to these three atoms, and the total four-body potential is calculated as a function of this variable separation distance, d_l. The four-body interaction is isolated from the two- and three-body contributions using the standard cluster expansion approach:

$$V_{4,ijkl} = V(d_l) - \sum_{i=1}^{4} V_{1,i} - 2\sum_{i=1}^{4}\sum_{j>i}^{4} V_{2,ij}(r_{ij})$$

$$- 2\sum_{i=1}^{N}\sum_{j\neq i}^{N}\sum_{k>j}^{N} V_{3,ijk}(r_{ij}, r_{jk}, \theta_{ijk}). \tag{14}$$

As shown in Fig. 3 for the Se_4 and Te_4 clusters, the four-body interaction is highly repulsive at short distances and rapidly decays to zero. We fit the *ab initio* data with

$$\frac{1}{4}V_4(d_l) = g \ \text{sech}(hd_l), \tag{15}$$

where g and h are constants and the factor of $\frac{1}{4}$ accounts for the contribution of four different four-body interactions to

TABLE IV. Parameters for the effective four-body interaction potential.

	Selenium	Tellurium
g (eV)	42	30
h (Å^{-1})	2.0	1.5

the total four-body potential. Values for g and h are given in Table IV for both the Se_4 and Te_4 clusters.

The case of a heterogeneous four-body cluster could become difficult given the number of different combinations of elements in different positions. We may dramatically simplify this case by assuming that the total four-body interaction is the sum of the four-body contributions of the individual elements in the cluster. For example, the four-body interaction for a Se_3Te cluster would be

$$V_4 = 3g_{Se} \ \text{sech}(h_{Se}d_l) + g_{Te} \ \text{sech}(h_{Te}d_l), \tag{16}$$

and the four-body interaction for a $SeTe_3$ cluster would be
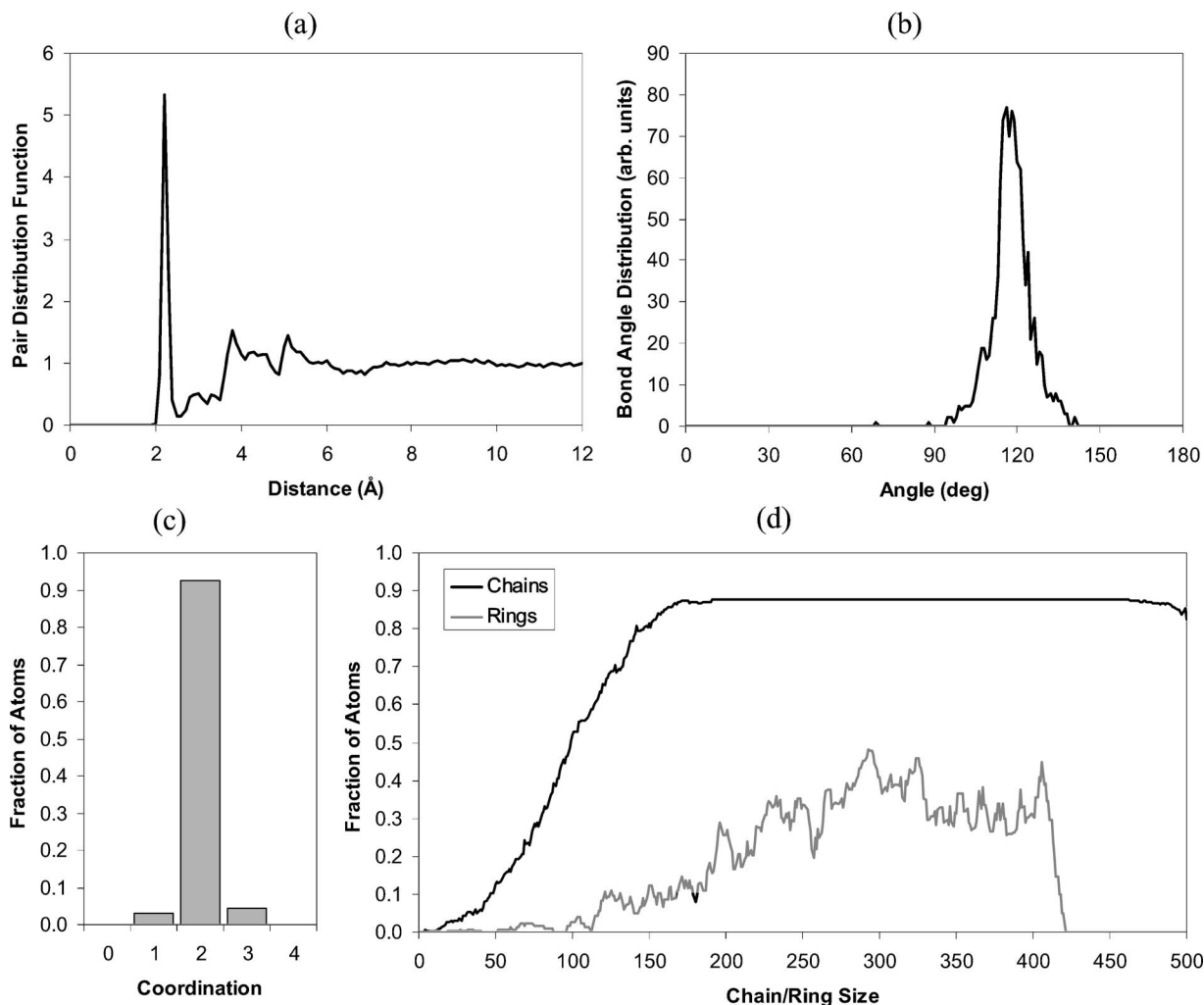
FIG. 4. Calculated structural data for Se glass assuming a density of 4.3 g/cm^3: (a) pair distribution function, (b) bond angle distribution, (c) coordination number distribution, and (d) chain or ring-length distributions.
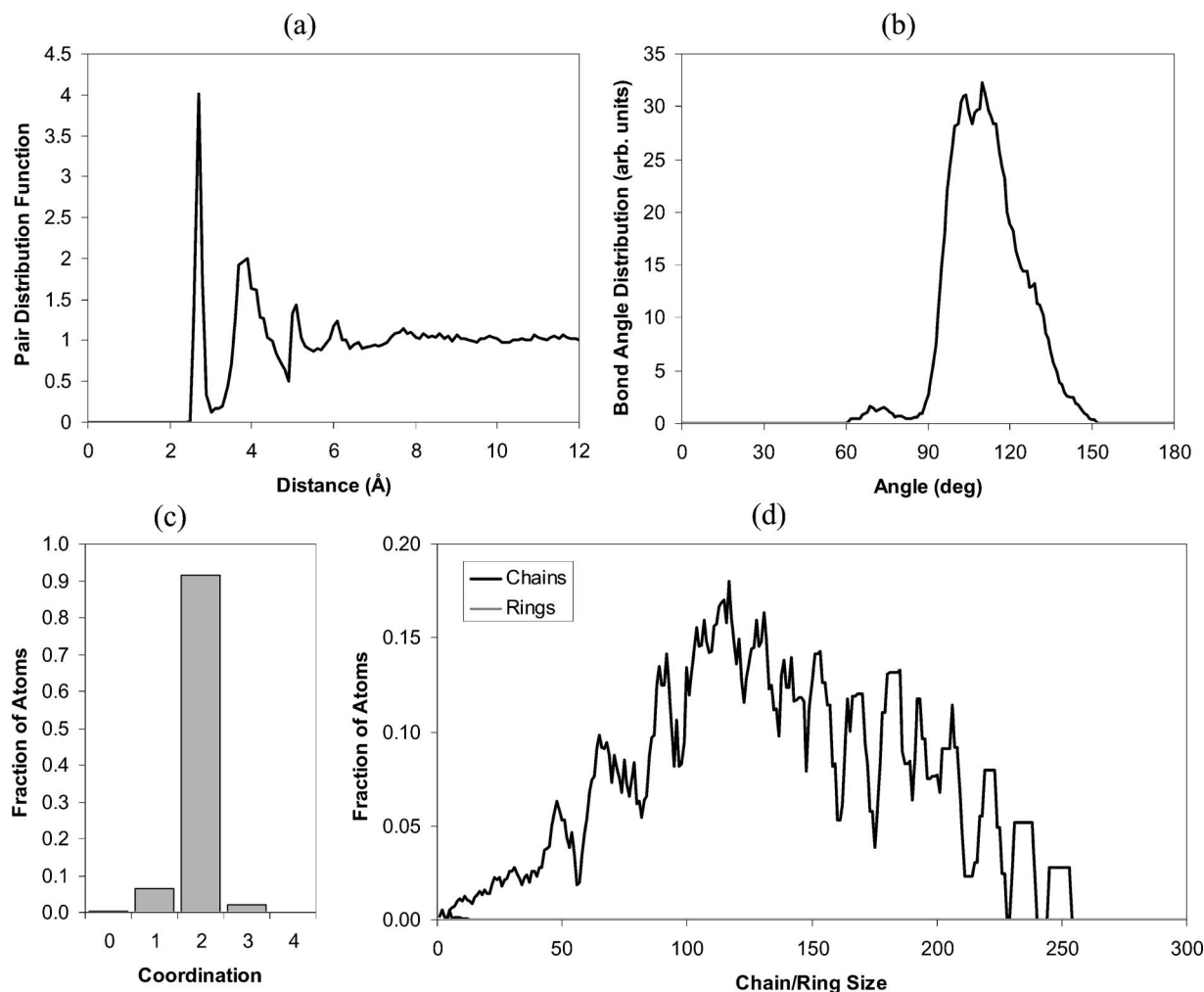
FIG. 5. Calculated structural data for Te glass assuming a density of 5.9 g/cm^3: (a) pair distribution function, (b) bond angle distribution, (c) coordination number distribution, and (d) chain or ring-length distributions.

$$V_4 = g_{Se} \operatorname{sech}(h_{Se}d_l) + 3g_{Te} \operatorname{sech}(h_{Te}d_l). \qquad (17)$$

We have previously demonstrated that this is a reasonable assumption and fits well to *ab initio* data for heterogeneous clusters of chalcogen elements.[28]

IV. MODELING OF GLASS STRUCTURE

In this section we use the recently developed interaction potentials combined with the Metropolis Monte Carlo molecular simulation technique[29,30] to model the structure of glasses in the Se$_x$Te$_{1-x}$ system. The simulations begin by placing 1000 atoms at random positions in a cubic, isochoric simulation space with periodic boundary conditions. The density of a Se$_x$Te$_{1-x}$ glass is assumed to be 5.9 $-1.6x$ g/cm^3, and we consider a constant temperature of $T = 298$ K. The trial displacements are made by assigning a random move along each of the three global axes, $\hat{\mathbf{x}}$, $\hat{\mathbf{y}}$, and $\hat{\mathbf{z}}$, where the probability density function is Gaussian with zero mean and a standard deviation of σ. We simulate a total of 20 million trial displacements of single atoms with a target acceptance rate of 40%. The magnitude of σ is dynamically

adjusted during the simulation to achieve this acceptance rate.

Since our cluster expansion approach to potential development is based on energies computed for small isolated clusters of atoms, it is desirable to test the validity of these potentials in an extended, three-dimensional solid. While we have accurately included interactions up to the fourth order, higher order interactions, if significant, could change the overall cohesive energy of a solid system. We have computed a cohesive energy of 2.258 eV/atom for pure selenium glass using our two-, three-, and effective four-body potentials. This is in excellent agreement with experimental values, which range from about 2.25 to 2.35 eV/atom, depending on the defect concentration in the glass.[31,32] Therefore, we may gain confidence in our cluster expansion method and the truncation of higher order interaction terms.

Figure 4 shows computed structural data for the case of a pure Se glass ($x = 1$). As discussed previously,[24] the structure of Se glass is dominated by long, two-coordinated chains of atoms. The pair distribution function in Fig. 4(a) agrees well with previous experimental and modeling work.[4,33–36] The bond angle, coordination number, and chain or ring-length distributions in Fig. 4(b)–4(d) assume a bond cutoff of 2.6 Å
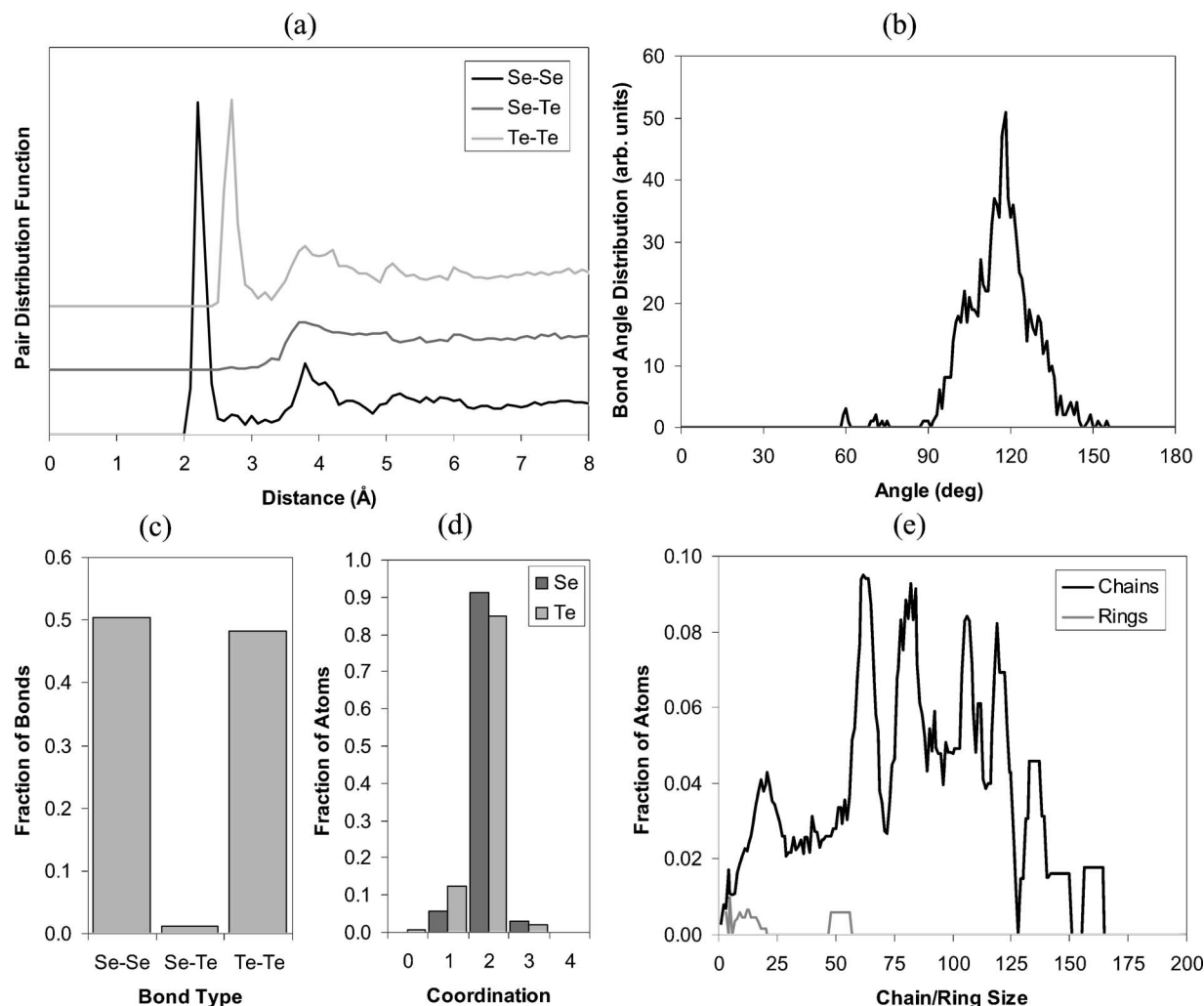
FIG. 6. Calculated structural data for $Se_{0.5}Te_{0.5}$ glass assuming a density of 5.1 g/cm^3: (a) pair distribution functions, (b) bond angle distribution, (c) bond population, (d) coordination number distribution, and (e) chain or ring-length distributions.

and are in good qualitative agreement with other experiments.[24,37–40] We find that 92.5% of atoms are two-coordinated, leading to chain lengths that approach the size of our simulated system. We also find the presence of large rings containing hundreds of atoms.

Similar structural data are shown in Fig. 5 for elemental Te glass. The pair distribution function in Fig. 5(a) predicts well-defined first and second neighbor distances and complete amorphism after about 8 Å. These features are in very good agreement with neutron scattering data[41] for liquid tellurium. The bond angle distribution in Fig. 5(b) consists of a broad peak centered around 110°. This distribution is significantly broader than for selenium. The coordination number distribution for Te glass is plotted in Fig. 5(c), assuming a bond cutoff distance of 3.0 Å. We find that 91.4% of atoms are two-coordinated, leading to long chains of atoms similar to that found in Se glass, a result which is in good qualitative agreement with neutron scattering studies.[42] Comparing Fig. 5(d) with Fig. 4(d), we note that the atomic chains in Te glass are significantly shorter than those in Se glass; moreover, ring structures are almost completely absent in Te glass.

Structural data for a $Se_{0.5}Te_{0.5}$ glass is provided in Fig. 6.

Whereas the homopolar pair distribution functions in Fig. 6(a) have strong first-neighbor peaks, the Se-Te pair distribution is zero until after 3 Å and shows very little correlation thereafter. This is a result of the glass's strong preference for homopolar bonding, shown in Fig. 6(c). Here we see that nearly 99% of all bonds are homopolar, indicating almost perfect phase separation at the covalent chain level. As shown in Fig. 6(d), the Se and Te atoms are primarily two-coordinated and there is a slightly higher number of miscoordinated atoms than in the elemental glasses, presumably due to the phase-separated nature of the heterogeneous glass. It follows that the chain lengths for $Se_{0.5}Te_{0.5}$ glass are shorter than for both elemental glasses, as indicated by Fig. 6(e). While there is not much experimental data on the $Se_{0.5}Te_{0.5}$ system available in literature, our structural data is in good qualitative agreement with the experimental predictions that the glass should consist of two-coordinated chains of atoms[43] and is phase separated.[44]

Fig. 7(a) plots the average coordination number of Se and Te atoms in Se_xTe_{1-x} glass as a function of x. We find that the average coordination number of Se drops with low Se content, as does the average coordination number of Te with low
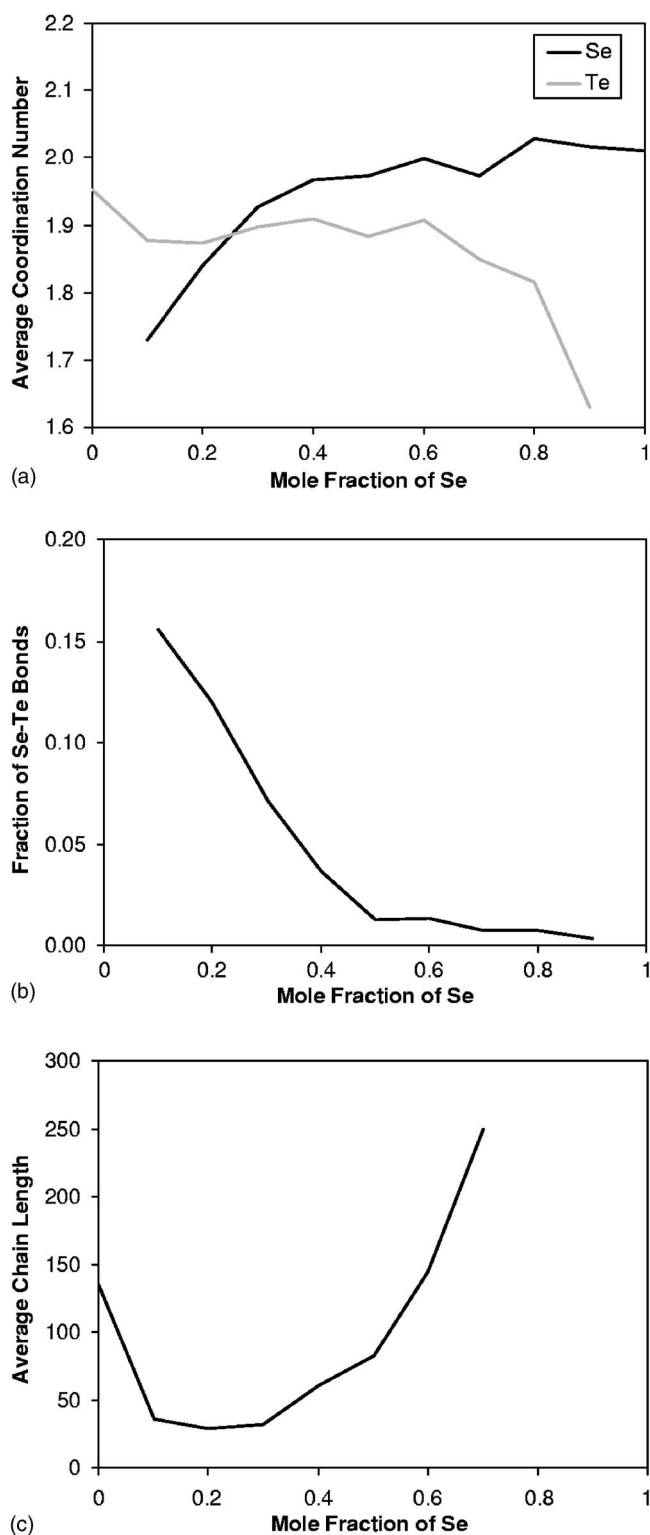
FIG. 7. Calculated structural data for glasses in the Se$_x$Te$_{1-x}$ system: (a) average coordination number, (b) fraction of heteropolar bonds, and (c) average chain length.

FIG. 8. (Color online) Computed structure (20 Å $\times$ 20 Å $\times$ 20 Å subset) of (a) Se$_{0.1}$Te$_{0.9}$ and (b) Se$_{0.9}$Te$_{0.1}$ glasses. The smaller (gray) atoms are Se, and the larger (blue) atoms are Te. These plots show that Se is more soluble in a high-Te glass than Te in a high-Se glass

Te content. Interestingly, Fig. 7 shows that the fraction of heteropolar bonds increases with decreasing Se content, indicating that Se is more soluble in a high-Te glass than Te in a high-Se glass. This can also be seen from the glass structure plots in Fig. 8. Combining these two findings, the aver-

age chain length should be a minimum for low Se-content glasses. This result is confirmed by Fig. 7(c), where we see that the average chain length is a minimum at about $x=0.2$. In addition, Fig. 7(b) shows that the fraction of Se-Te bonds becomes exceedingly small for $x \gtrsim 0.4$, indicating a high degree of phase separation in this regime.

V. CONCLUSIONS

We have developed model interaction potentials for the binary selenium-tellurium system based on Møller-Plesset perturbation theory. The model potentials successfully reproduce the two-coordinated chainlike structure of glasses in the Se_xTe_{1-x} system. Heterogeneous Se_xTe_{1-x} glasses are found to be phase separated for $x \gtrsim 0.4$. The minimum average chain length occurs around $x=0.2$.

[1] A. K. Varshneya, J. Non-Cryst. Solids **273**, 1 (2000).

[2] C. Oligschleger, R. O. Jones, S. M. Reimann, and H. R. Schober, Phys. Rev. B **53**, 6165 (1996).

[3] F. H. Stillinger, T. A. Weber, and R. A. LaViolette, J. Chem. Phys. **85**, 6460 (1986).

[4] D. Caprion and H. R. Schober, Phys. Rev. B **62**, 3709 (2000).

[5] C. Oligschleger and J. C. Schön, J. Phys.: Condens. Matter **9**, 1049 (1997).

[6] C. Oligschleger and H. R. Schober, J. Non-Cryst. Solids **250-252**, 651 (1999).

[7] D. Caprion and H. R. Schober, J. Chem. Phys. **117**, 2814 (2002).

[8] D. Caprion and H. R. Schober, J. Non-Cryst. Solids **326-327**, 369 (2003).

[9] C. J. Cramer, *Essentials of Computational Chemistry: Theories and Models* (Wiley, West Sussex, U.K., 2002).

[10] F. Shimojo, K. Hoshino, M. Watabe, and Y. Zempo, J. Phys.: Condens. Matter **10**, 1199 (1998).

[11] F. Shimojo, K. Hoshino, and Y. Zempo, J. Phys.: Condens. Matter **11**, 8829 (1999).

[12] F. Shimojo, K. Hoshino, and Y. Zempo, J. Non-Cryst. Solids **312-314**, 290 (2002).

[13] X. Zhang and D. A. Drabold, Phys. Rev. Lett. **83**, 5042 (1999).

[14] X. Zhang and D. A. Drabold, Int. J. Mod. Phys. B **15**, 3190 (2001).

[15] O. F. Sankey and D. J. Niklewski, Phys. Rev. B **40**, 3979 (1989).

[16] F. Shimizu, H. Kaburaki, T. Oda, and Y. Hiwatari, J. Non-Cryst. Solids **250-252**, 433 (1999).

[17] K. Nakamura and A. Ikawa, Phys. Rev. B **67**, 104203 (2003).

[18] R. Stadler and M. J. Gillan, J. Phys.: Condens. Matter **12**, 6053 (2000).

[19] C. Møller and M. S. Plesset, Phys. Rev. **46**, 618 (1934).

[20] A. K. Wilson, D. E. Woon, K. A. Peterson, and T. H. Dunning, Jr., J. Chem. Phys. **110**, 7667 (1999).

[21] K. A. Peterson, D. Figgen, E. Goll, H. Stoll, and M. Dolg, J. Chem. Phys. **119**, 11113 (2003).

[22] GAUSSIAN 03 , Revision B.04, Gaussian, Inc., Pittsburgh 2003.

[23] K. Huang, *Statistical Mechanics* (Wiley, New York, 1987), ch. 10.

[24] J. C. Mauro and A. K. Varshneya, Phys. Rev. B **71**, 214105 (2005).

[25] P. M. Morse, Phys. Rev. **34**, 57 (1929).

[26] P. Schwerdtfeger, J. R. Brown, J. K. Laerdahl, and H. Stoll, J. Chem. Phys. **113**, 7110 (2000).

[27] K. Nagaya, A. Oohata, I. Yamamoto, and M. Yao, J. Non-Cryst. Solids **312-314**, 337 (2002).

[28] J. C. Mauro and A. K. Varshneya, *6th Pacific Rim Conference on Ceramic and Glass Technology* (American Ceramic Society, , 2005).

[29] N. Metropolis, A. W. Rosenbluth, M. N. Rosenbluth, A. H. Teller, and E. Teller, J. Chem. Phys. **21**, 1087 (1953).

[30] M. N. Rosenbluth and A. W. Rosenbluth, J. Chem. Phys. **22**, 881 (1954).

[31] D. Vanderbilt and J. D. Joannopolous, Phys. Rev. B **22**, 2927 (1980).

[32] D. Vanderbilt and J. D. Joannopolous, Phys. Rev. B **27**, 6296 (1983).

[33] K. Tamura and S. Hosokawa, Ber. Bunsenges. Phys. Chem. **96**, 681 (1992).

[34] D. Molina, E. Lomba, and G. Kahl, Phys. Rev. B **60**, 6372 (1999).

[35] P. Jóvári, R. G. Delaplane, and L. Pusztai, Phys. Rev. B **67**, 172201 (2003).

[36] J. Hegedüs, K. Kohary, and S. Kugler, J. Non-Cryst. Solids **338-340**, 283 (2004).

[37] E. Billig, Proc. Phys. Soc. London, Sect. B **65**, 216 (1952).

[38] K. Tamura, J. Non-Cryst. Solids **205-207**, 239 (1996).

[39] K. M. Bernatz, I. Echeverría, S. L. Simon, and D. J. Plazek, J. Non-Cryst. Solids **307–310**, 790 (2002).

[40] K. Nakamura and A. Ikawa, J. Non-Cryst. Solids **312–314**, 168 (2002).

[41] G. Tourand, B. Cabane, and M. Breuil, J. Non-Cryst. Solids **8–10**, 676 (1972).

[42] A. Chiba, Y. Ohmasa, Y. Kawakita, M. Yao, and H. Endo, J. Non-Cryst. Solids **312–314**, 384 (2002).

[43] L. M. Needham, M. Cutroni, A. J. Dianoux, and H. M. Rosenberg, J. Phys.: Condens. Matter **5**, 637 (1993).

[44] D. Lezal, J. Optoelectron. Adv. Mater. **5**, 23 (2003).